Journal of Applied Mechanics Vol.10, pp.983-994 (August 2007) JSCE

A HEALTH MONITORING STRATEGY FOR RC FLEXURAL STRUCTURES BASED ON DISTRIBUTED LONG-GAGE FIBER OPTIC SENSORS

Suzhen LI[1], Zhishen WU[2] and Watanabe TAKUMI[3]

[1]PhD. student, Dept. of Urban and Civil Engineering, Ibaraki University
(Nakanarusawa-cho 4-12-1, Hitachi, Ibaraki 316-8511, Japan)
Currently work at Colloege of Civil Engineering, Tongji University, Shanghai, China
E-mail:Lszh99@gmail.com
[2]Professor, Dept. of Urban and Civil Engineering, Ibaraki University
(Nakanarusawa-cho 4-12-1, Hitachi, Ibaraki 316-8511, Japan)
E-mail:zswu@mx.ibaraki.ac.jp
[3]Master student, Dept. of Urban and Civil Engineering, Ibaraki University
(Nakanarusawa-cho 4-12-1, Hitachi, Ibaraki 316-8511, Japan)
E-mail: takumisan8@yahoo.co.jp

RC structural health monitoring (SHM) often includes two main concerns on local damage detection and global structural behavior. In our recent study, a novel packaged long-gage fiber Bragg grating (FBG) sensor for practical adaptation in civil SHM has been developed and verified to have the ability to obtain effective macro-strain distributions. This paper is dedicated to proposing an integrated SHM strategy for RC flexural structures by employing the developed sensors. Experimental investigations on a normal RC beam installed with the FBG sensors of different gauge length are first carried out. On one hand, the ability of distributed FBG sensors to detect the occurrence, location and extent of cracks has been testified in contrast with the results from foil strain gauges and crack gauges. On the other hand, a perfect linear correlation between the measurements from FBG sensors and those from displacement transducers has testified the sound performance of the developed sensors for global structural behavior evaluation. Numerical simulations based on section fiber modeling method with the plane section assumption are then performed to compare with the experimental results. Their nice agreements have further verified the ability of the FBG sensors to estimate structural parameters and evaluate structural global behavior. Regarding these meaningful investigations, the inverse analysis including load and structural parametric identification is carried out by utilizing the measured macro-strain distribution. An integrated SHM strategy based on distributed long-gage FBG sensors for RC flexural structures including local crack monitoring, parametric estimation and global behavior evaluation is proposed finally.

Key Words : *distributed long-gage fiber optic sensors, RC structures, health monitoring, local crack monitoring , parametric estimation, global behavior evaluation*

1. INTRODUCTION

Health monitoring for RC structures often includes two main concerns on local damage detection and global structural behavior. Cracks may lead to structural degradation due to reinforcement corrosion associated with the leakage of water and chloride through cracks. Therefore, the damage detection including the monitoring on the presence, location and significance of cracks, reinforcement corrosion, material behaviors or local stress/strain concentrations and so on is of engineering significance concerning maintenance and reparation of concrete structures in service as well as after the occurrence of natural hazards. On the other hand, the global behavior evaluation provides the valuable macroscopic information on the full structural assessment and diagnosis.

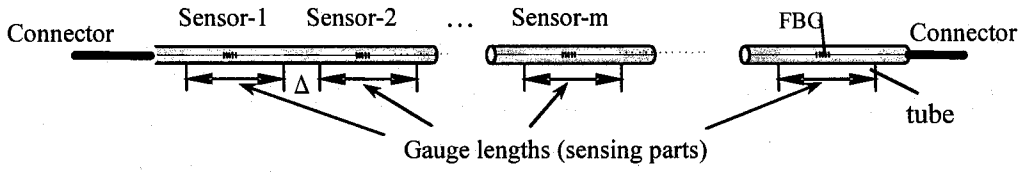

Fig.1 Long-gage FBG sensors array

Different from visual observation inspection, the real-time monitoring by directly using measurements has drawn the extensive interests regarding its fewer requirements for labor, more convenience for in-service structural monitoring and the ability to obtain the immediate information. To overcome the difficult in traditional transducers such as the problems of installation, durability, stability and so on, some novel sensing techniques are employed for RC structural health monitoring. Fiber optic sensing technologies under rapid development in the recent years have drawn extensive interests and are expected to be achievements in the innovation of sensing techniques. Especially, FBG sensor, which in nature holds high precision and dynamic measuring ability, has been supposed to be one of the most promising fiber optic sensor. Although many works[1)2)3)] have drawn attention to the practical application of FBG sensor in civil structures and some projects have brought it from laboratory to field, most of them focused on the usage of FBG sensor as a localized gauge for point or axial strain measurements and the integrated methodology for structural health monitoring (SHM) based on the developed sensor is scarely any. In our recent study, a novel packaged long-gage fiber optic sensor for practical adaptation in civil structural health monitoring has been developed and verified to have the ability to obtain effective macro-strain distributions[4)]. Meanwhile, the concept of distributed strain sensing techniques is proposed[5)], which has been dedicated to utilizing the strain distributions throughout the full or some partial areas of structures to detect the arbitrary and unforeseen damage.

In this regards, the application of the developed long-gage FBG sensor in health monitoring for RC flexural structural is discussed. A normal RC beam installed with distributed FBG sensors of different gauge lengths are utilized for experimental investigations, in which progressing cracks are introduced in successive loading steps and respective measurements from FBG sensors are obtained. Numerical simulations based on section fiber modeling method are then performed to compare with the experimental results. Combined with the investigations on experiments and simulations, the inverse analysis including load and structural parametric identification is carried out by utilizing the measured macro-strain distribution. An integrated SHM strategy based on distributed long-gage FBG sensors for RC flexural structures including local crack monitoring, parametric estimation and global behavior evaluation is proposed finally.

2. LONG-GAGE FBG SENSORS ARRAY FOR DISTRIBUTED MACRO-STRAIN MEASUREMENTS

A long-gage FBG sensor has been developed recently in our lab for practical adaptation to civil structures. The essential of this sensor (see **Fig.1**) is the handling of an embedded tube, inside which bare optic fiber with FBG is sleeved and fixed at two ends. Through special packaging by composite materials to extend original Bragg grating with inherent gage lengths on the order of a few millimeters to effective gauge length up to several centimeters or meters, FBG sensor can measure the average macro-strain that is less susceptible to local stress/strain concentrations and hence more representative of the deformation of the entire structural member. Furthermore, compared with resistive foil strain gauge and other traditional "point" gauges, this sensor can be easily multiplexed at many locations or distributed throughout the full structure and permit distributed strain measurements of high precision. The image of distributed long-gage FBG sensors array can be seen in **Fig.1**. It is worth stressing here that in our design the "zero" distance (Δ=0) between two FBG sensors can be implemented and a real distributed measurement can be achieved.

Single-mode optical fiber of Corning SMF-28 was utilized in this study. All the FBGs available for commerce passed 100KPSI proof test and basically could be used to measure strains up to 5000με repeatedly.Meanwhile, an FBG-Interrogation system from NTT-AT with sampling rate of 50Hz was used for data acquisition and signal interpretation.

3. EXPERIMENTAL INVESTIGATIONS

3.1 Test specimen and sensors placement

A RC beam with rollers supported at two points is designed as the test specimen. The total length of the beam is 2.1m, with a span of 1.8m. The cross section has a rectangular shape with 150mm width and 200mm depth. The compressive strength of concrete is 45.6 N/mm^2. Two positive reinforcements of 16mm diameter and two passive ones of 13mm diameter are used for longitudinal bars, with 40 mm distance away from the edges of the beam. Stirrups are also considered throughout the whole length of the specimen, with 10mm diameter and 80mm distance at two adjacent vertical bars. The yield strength of reinforcement is 380 N/mm^2. The failure mode of the beam is flexural failure in the design.

Via a transferred steel board, the load applied by loading machine is equivalently split into two parts, landing at two points with a distance of 600mm (corresponding to 1/3 of the span) from each support. The progressively increasing load is applied continuously in a load-controlled mode, up to the failure of beam. To detect the subtle changes before and after the first several cracks, upload is carried out at a very low speed before 30 KN, where 15 KN is supposed to be the cracking load from theoretical calculation.

To study the performance of long-gage strain sensors on structural assessment for RC beam, four FBG sensors of 200mm gauge length are arranged onto the bottom surface of the specimen to implement a quasi-distributed measurement. The other two kinds of FBG sensors with respective gauge length of 400mm and 800mm are attached in parallel to investigate the influence of different gauge lengths on the sensor behavior. Traditional foil strain gauges of 60mm gauge length are fixed at the top, bottom and side surfaces of the beam. Crack gauges of 200mm gauge length are also used for comparison. A displacement gauge is installed at the center of the specimen to provide an index to verify the structural global behavior. For the convenience of discussion, the area with sensors installation is artificially divided into four zones, as denoted by Zone1~Zone4. The specimen and sensors placement are described in details in **Fig.2**.

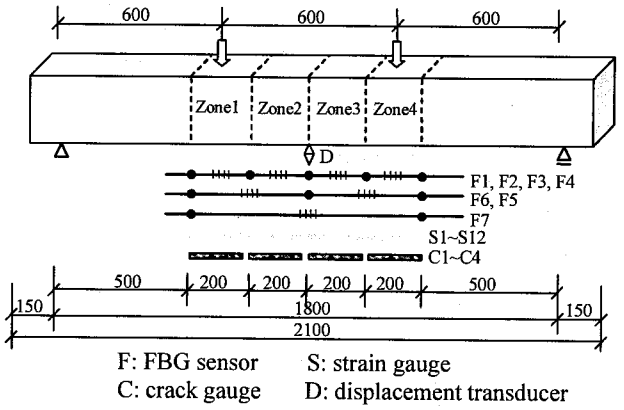

Fig.2 Sensors placement

3.2 Experimental results

As mentioned before, upload is applied at a very low speed from the beginning and all of the sensors work in a good condition with graphically linear increases under load. The first abrupt change of the data can be found from S8 in Zone 2 at 13KN, when the initial crack is supposed to occur. With the going-up load, cracks occur and propagate in succession at different locations where the spatial space between two cracks is about 100mm. As the load is up to 35KN, five FBG sensors including [F1, F2, F3, F4, F5] fail to work. The accidental reason is still under investigation and likely in that F2 encoded by center wavelength of 1538nm got some problem and incurred the mistaken interrogation of the following [F1, F3, F4, F5] encoded by their respective center wavelengths of [1538nm,1540nm, 1550nm, 1552nm]. Otherwise, F6 (1535nm) and F7 (1532nm) work well

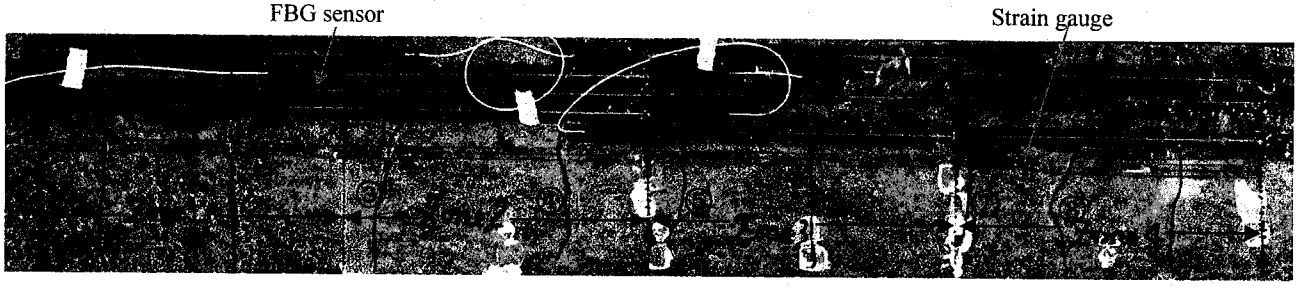

Fig.3 Crack distribution at the bottom surface after experiment

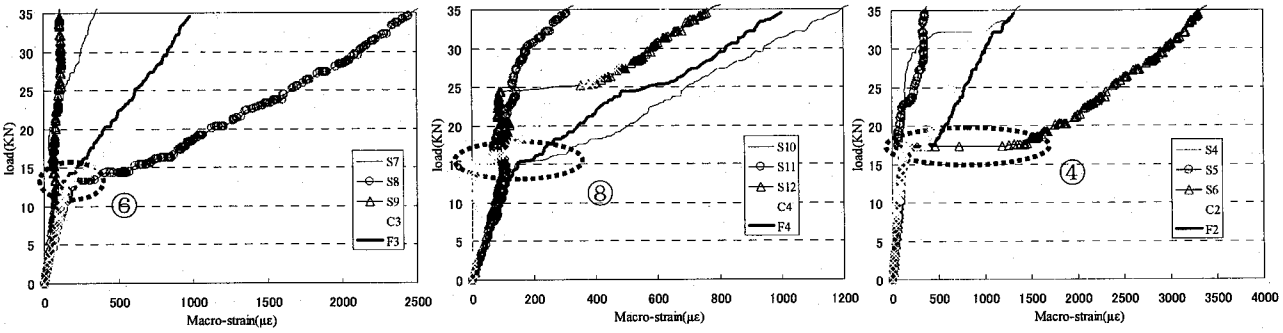

(1) Crack ⑥ (first crack) (2) Crack ⑧ (second crack) (3) Crack ④(third crack)

Fig.4 Crack locating

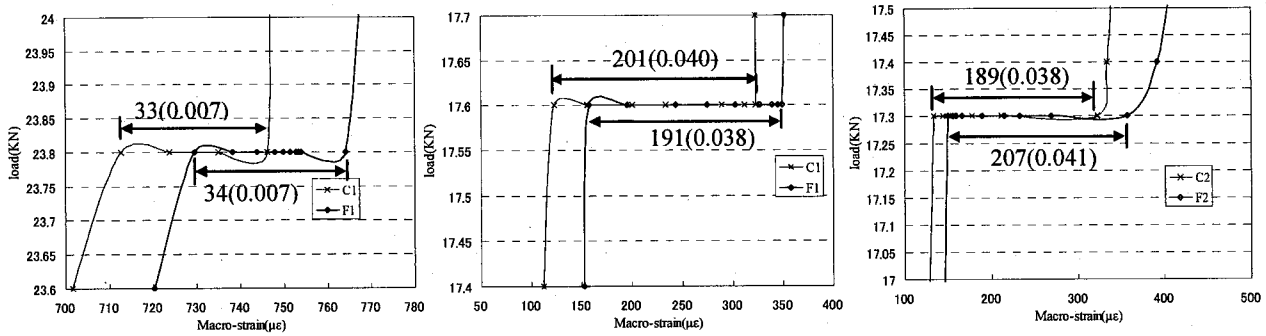

(1) Crack ① (2) Crack ② (3) Crack ④

* Macro-strain (Average crack width) Unit: με (mm)

Fig.5 Average crack width

until the end of the experiment, when the load is about 75KN. The outline of the specimen after the experiment is shown in **Fig. 3**. For the convenience of the following description, the cracks at the bottom surface of the beam are labeled ①~⑨ from left to right.

(1) Local crack monitoring

Cracks detection and localization The strain measurements with loading increase from FBG sensors of 200mm gauge length are shown in **Fig. 4**. It can be found that the first three cracks of the beam can be detected easily by FBG sensors from both the inflection points after which the slopes of the curves decrease discontinuously and the abrupt increase of measured macro-strains under the constant load.

Average crack width The average crack width within a certain region (i.e. the actural crack width devided by sensor gauge length) can be regarded as the product of the increase of measured macro-strains and the gauge length of the sensor under the constant load. Considering Zone 1 and Zone 2, the changes of measured data and the corresponding average crack widths obtained by crack gauges and FBG sensors of 200mm gauge length are shown in **Fig. 5**. In the cases (crack①②④) the results from these two different sensors present a good agreement.

Influence of gauge lengths of sensors on crack monitoring Four kinds of long-gage strain sensors are utilized in this study, including the strain gauge of 60mm gauge length and three FBG sensors of 200mm, 400mm, 800mm gauge lengths. Considering the cracks ⑥⑧④ which are the first three cracks of the beam in this experiment, the comparative measured results from the above four long-gage sensors can be seen in **Fig.6**. Obviously with the increase of the gauge length of the sensor, the measured macro-strains change less when the crack occurs, which has proven a very important concept that the average macro-strain is less susceptible to the local stress /strain concentration and more representative of the deformation of the entire structural member. Furthermore, it can be concluded that as long as the extent of crack is small or the gauge length of the sensor is large enough, the aberrant changes in the measured data caused by local crack can be reduced to keep the continuity of the final results.

(2) Global structural behavior

The macro-strain responses obtained by F6 and F7 under monotonic loads are shown in **Fig. 7** (1). Basically, the behavior of the RC beam including

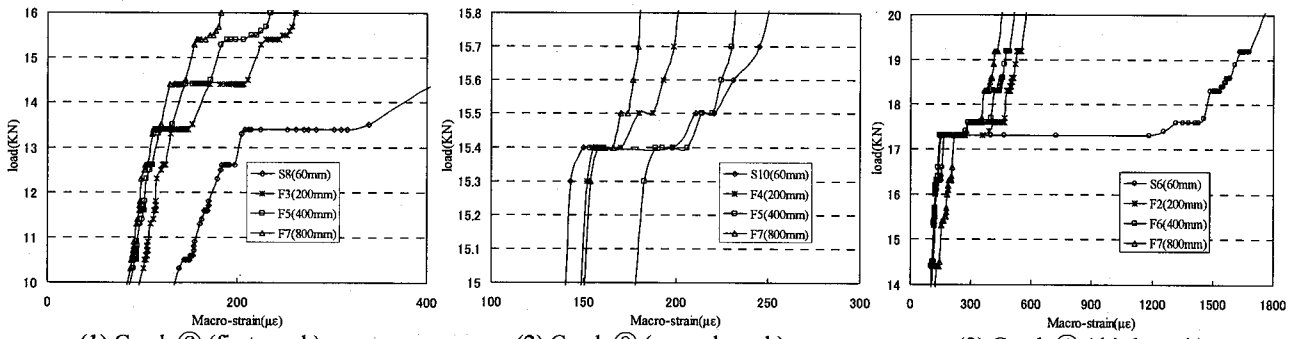

(1) Crack ⑥ (first crack) (2) Crack ⑧ (second crack) (3) Crack ④ (third crack)

Fig.6 Crack monitoring based on strain sensors of different gauge lengths

initiation of first crack and yielding of rebars are reflected effectively. In general, for such a RC beam with the final crack spatial space of about 100mm, the measurements from the FBG sensor of 200mm or larger gauge length can disregard the influence of local crack and reflect the structural macro-behavior well. On the other hand, the macro-strain vs. deflection curves are illustrated in **Fig.7** (2), where a perfect linear correlation can be obtained before the yielding of tensile bars. This conclusion is very valuable for the reason that if the gauge length and location of the sensors are selected reasonably, the long-gage FBG sensors can replace the displacement transducers which are often used for global deflection measurements but difficult to be installed onto the practical civil structures due to the requirement for baseline position. Moreover, it can be seen that the correlation curves maintain the sound accordance before and after cracking, which has again proved the above-mentioned argument that the FBG sensor with enough gauge length can obtain the measurements overlooking the influence of local crack.

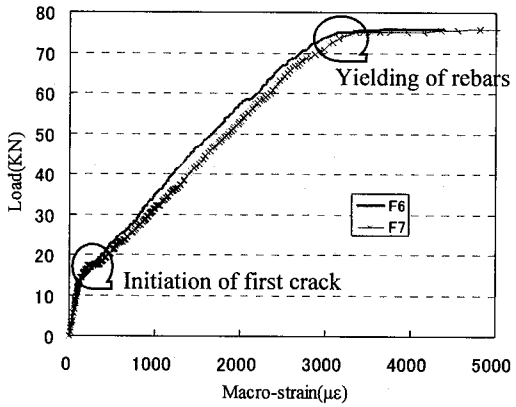

(1) Load vs. macro-strain curves

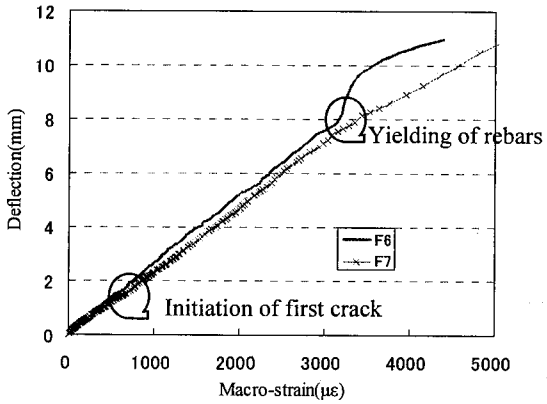

(2) Deflection vs. macro-strain curves

Fig.7 Macro-strain measurements from F6, F7

To investigate the effectiveness of the average of measured macro-strains, the comparative results from different gauge lengths are illustrated in **Fig.8**. The very satisfied agreements verify the conclusion that regarding RC beam the macro-strain measurements over a certain gauge length can be obtained from the average of those over several sub gauge lengths, i.e. the four distributed FBG sensors of 200mm gauge length are enough for global behavior evaluation on this RC beam. Together with the discussions from local crack monitoring, it can be found that the FBG sensor of 200mm gauge length is a good choice for a RC beam of about 2m span on structural assessment.

4. NUMERICAL SIMULATIONS

In view of global structural behavior evaluation rather than the initiation and propagation of local cracks, numerical nonlinear analysis based on section fiber modeling method are carried out in terms of the class bending theory with plane section assumption to establish the clear relations of various physical parameters for the sake of the later inverseanalysis on structural parametric estimation and performance evaluation.

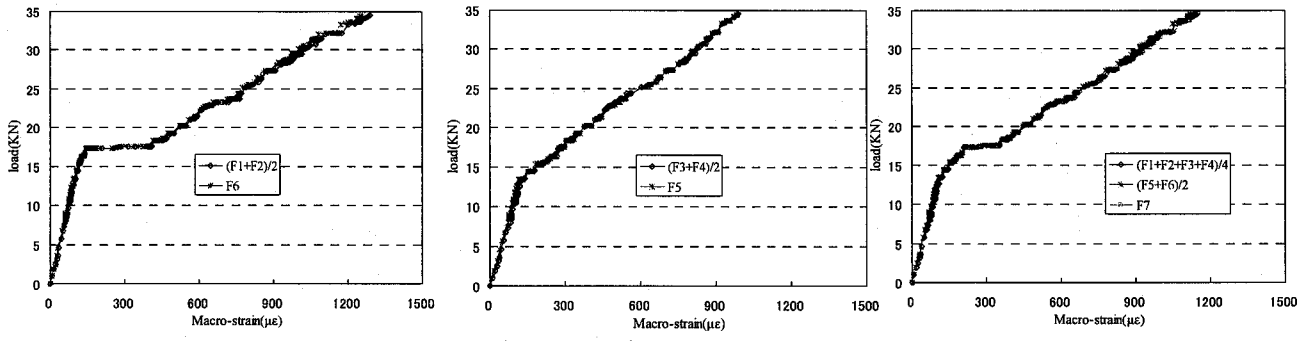

Fig.8 The average of macro-strain measurements

4.1 Material models

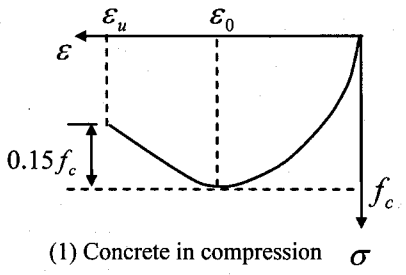

(1) Concrete in compression

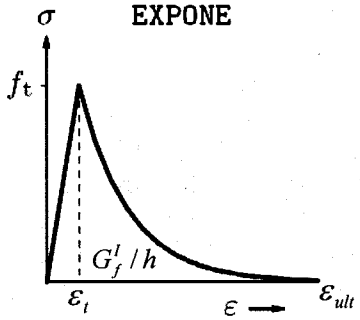

(2) Concrete in tension

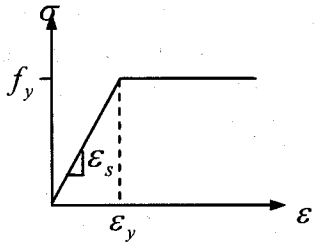

(3) Reinforcement

Fig.9 Material models

(1) Concrete models

Concrete in compression Concrete in compression is modeled by constitutive model suggested by Hognestad, which gives the stress in terms of strain in **Fig.9**(1) and Eq.(1). The same concrete compressive strength as that in experiments for $f_c = 45.6N/mm^2$ is adopted in the analysis.

$$\sigma = \begin{cases} f_c\left[\dfrac{2\varepsilon}{\varepsilon_0} - \left(\dfrac{\varepsilon}{\varepsilon_0}\right)^2\right] & \text{if } \varepsilon_0 < \varepsilon \le 0 \\ f_c\left[1 + \dfrac{0.15(\varepsilon - \varepsilon_0)}{\varepsilon_0 - \varepsilon_u}\right] & \text{if } \varepsilon_u \le \varepsilon < \varepsilon_0 \\ 0 & \text{if } \varepsilon \le \varepsilon_u \end{cases} \quad (1)$$

where $\varepsilon_0 = \dfrac{2f_c}{E}$, $\varepsilon_u = 0.0033$, E is the initial modulus of concrete.

Concrete in tension Concrete in tension before cracking is supposed to be linear elastic. After cracking however, a softening branch forms and it is assumed that the descending path follows an exponential function of crack width derived experimentally by Hordijk (1991). The constitutive models can be found in **Fig.9** (2), as shown in the following equations.

$$\begin{cases} \sigma = E \cdot \varepsilon & \text{if } \varepsilon \le \varepsilon_t \\ \dfrac{\sigma}{f_t} = \left(1 + \left(c_1 \dfrac{\varepsilon - \varepsilon_t}{\varepsilon_{ult} - \varepsilon_t}\right)^3\right)\exp\left(-c_2 \dfrac{\varepsilon - \varepsilon_t}{\varepsilon_{ult} - \varepsilon_t}\right) & \\ \quad - \dfrac{\varepsilon - \varepsilon_t}{\varepsilon_{ult} - \varepsilon_t}(1 + c_1^3)\exp(-c_2) & \text{if } \varepsilon_t < \varepsilon \le \varepsilon_{ult} \\ \sigma = 0 & \text{if } \varepsilon > \varepsilon_{ult} \end{cases} \quad (2)$$

where $\varepsilon_{ult} = \varepsilon_t + 5.136\dfrac{G_f^I}{hf_t}$, tensile fracture energy $G_f^I = 100N/m$, C_1=3, C_2=6.93. The concrete tensile strength for $f_t = 2N/mm^2$ is chosen to match the experimental result.

(2) Reinforcement model

Reinforcing steels are treated as a linear elastic-perfectly plastic material, as shown in

Fig.9(3). The same reinforcement compressive strength as that in experiments for $f_y = 380N/mm^2$ is adopted.

4.2 Section fiber model

Based on the assumption that plane sections remain plane and normal to the longitudinal axis, the nonlinear behavior of RC beam disregarding shear and bond-slip can derive from the constitutive relations of concrete and reinforcing steel fibers into which each section is divided, as shown in **Fig.10**.

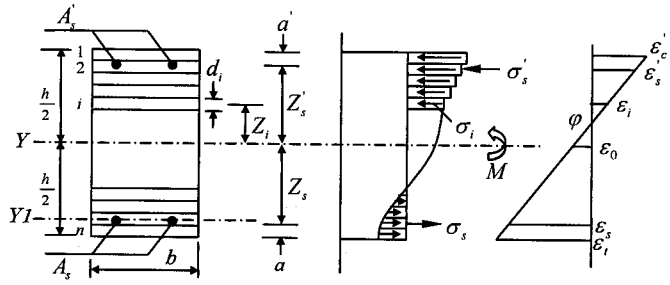

Fig.10 Section fiber model

Regarding one section, suppose the curvature φ and the strain ε_j at a point (or say "fiber") are known, and in term of them the strain throughout the whole section can be represented as

$$\varepsilon_i = f(\varphi, \varepsilon_j, Z_i) \tag{3}$$

Where $f()$ is a linear function. In **Fig.10**, $\varepsilon_j = \varepsilon_0$ is the strain at the geometric center of the section. Obviously,

$$\sum N = \sum_{i=1}^{n} \sigma_i A_i + \sigma_s A_s + \sigma_s' A_s' \tag{4}$$

$$\sum M = \sum_{i=1}^{n} \sigma_i A_i Z_i + \sigma_s' A_s' \left(\frac{h}{2} - a'\right) + \sigma_s A_s \left(\frac{h}{2} - a\right) \tag{5}$$

4.3 Nonlinear analytical scheme

Although Section fiber modeling is not a new method, the nonlinear analytical procedure is described briefly as follows to clarify the relations of various physical quantities such as load, structural parameters and macro-strain measurements for the later inverse analysis

(I) Calculate the moment vs. curvature relation for each section

(a). Take the curvature increment $\Delta\varphi$ for each step

(b). Assume an initial value of ε_0, the strain at the geometric center of the section

(c). Calculate the strain for every fiber over the whole section based on **Eq.(3)**

(d). Calculate the stress in terms of the strain from (c) and the material model in **Sec.4(1)**

(e). the gross interior force can be hence obtained from **Eq.(4)** to be used to check if the equilibrium condition is satisfied

(f) If $\sum N \neq 0$, ε_0 should be adjusted and (c) ~ (e) are iterative

(g) If $\sum N = 0$, the interior moment in terms of the curvature can be calculated .

(h) Repeat (a) ~ (g) until $\varepsilon_c' = \varepsilon_u$.

(II) For a beam with the given moment distribution throughout its length, the curvature distribution and hence the macro-strain can be obtained according to (I).

(III) To study the structural global behavior, the deflection distribution for the beam can be calculated based on the conjugated beam method and the known curvature distribution.

4.4 Analytical results

(1) Macro-strain responses under the same load pattern as that in experiments

Fig.11 gives the comparative results of the whole process of macro-strain responses from the experiments and simulations. It can be seen in **Fig.11**(1) that the measurements from FBG sensors

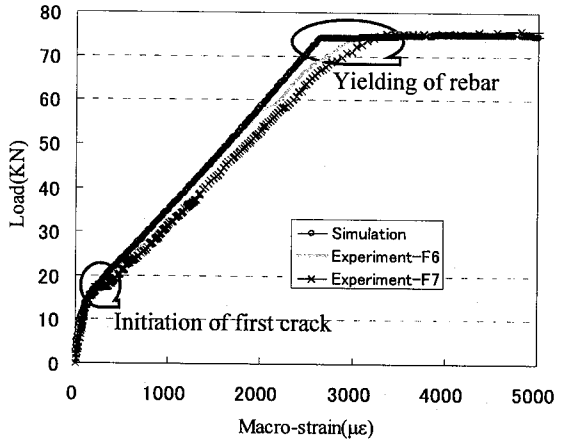

(1) Load vs. macro-strain curves

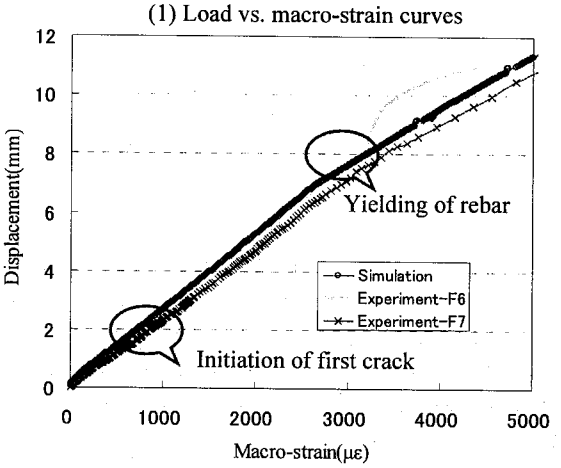

(2) Displacement vs. macro-strain curves

Fig.11 Macro-strain responses from F6, F7

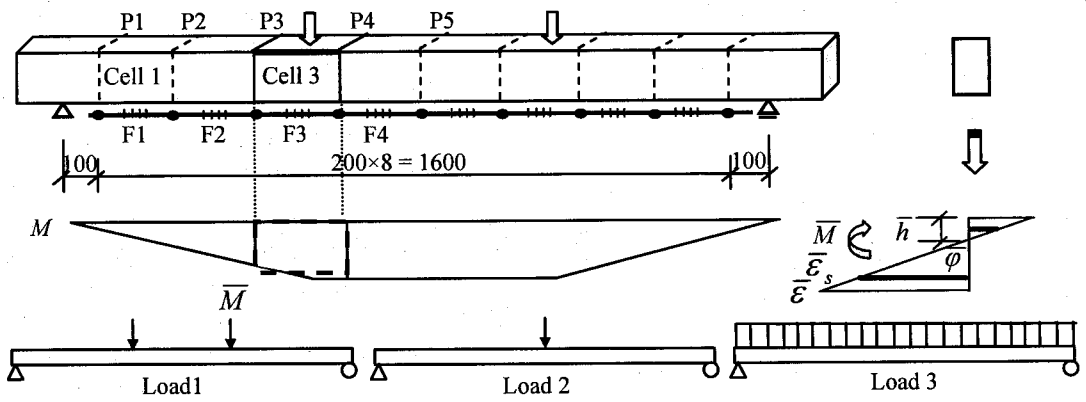

Fig.12 RC beam with eight FBG sensors and various load cases

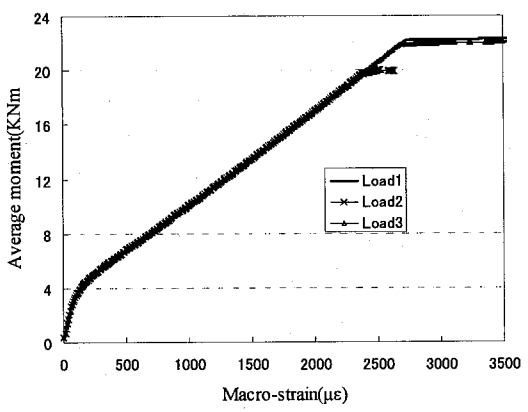

(1) Responses from F4 in different load cases

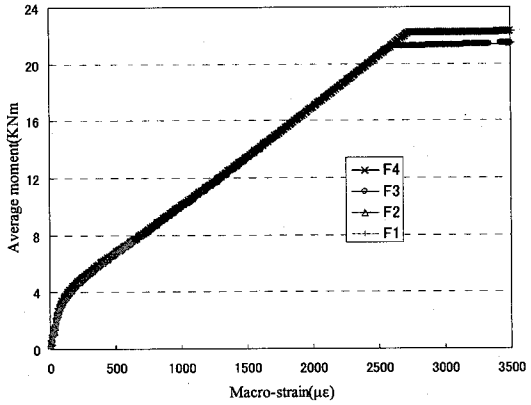

(2) Load 1

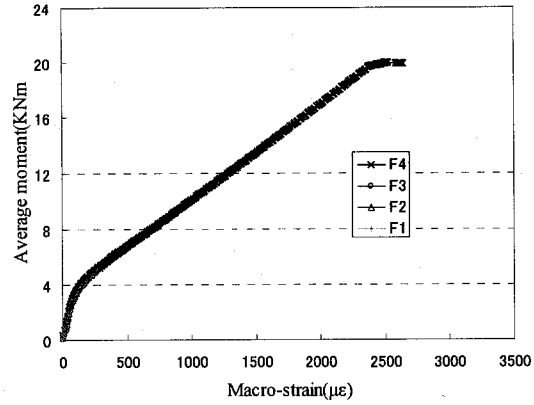

(3) Load 2

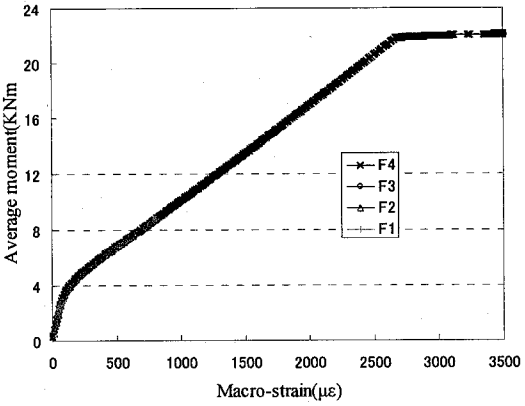

(4) Load 3

Fig.13 Average moment vs. macro-strain curves

match well with the analytic results before the initiation of the first cracks and have a close agreement with those after cracking. **Fig.11(2)** has further verified the important conclusion that there is a perfect linear correlation between macro-strain and displacemnt at mid-span of the beam.

(2) Average moment vs. macro-strain under different load patterns

Considering a same RC beam with eight distributed long-gage FBG sensors as shown in **Fig.12**, the relationships of average moment vs. macro-strain response under various load pattern including two-point, single-point and uniform distributed loads are investigated based on the section fiber model.

Taking the case of F4 measurement for example, as shown in **Fig.13**(1), the curves of average moment vs. macro-strain over the gauge length of F4 have a nice agreement under different load patterns except the responses after the yielding of reinforcing steel. Furthermore in each load case (see **Fig.13**

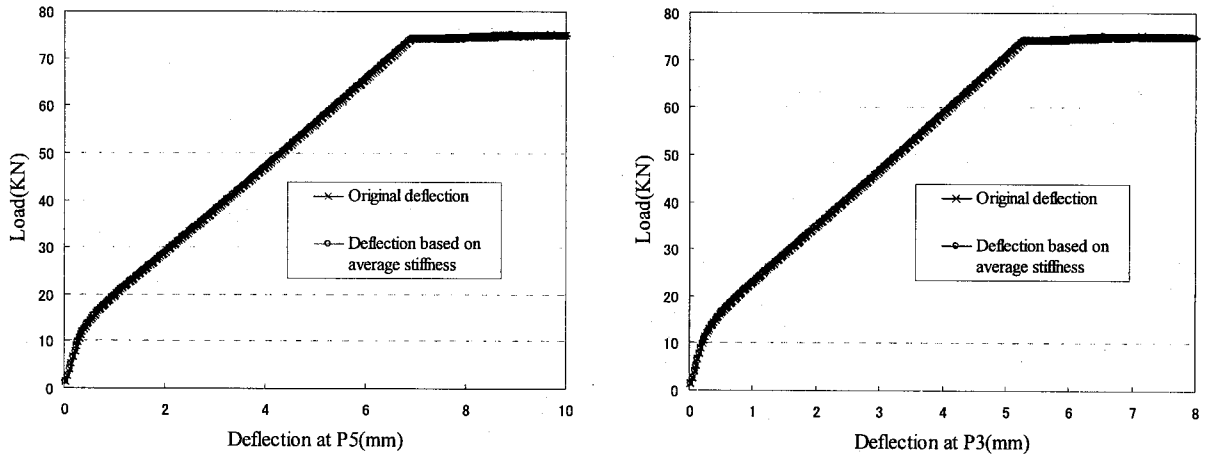

Fig.14 Deflection based on average stiffness in cells

(2)-(4)), the results from various FBG sensors have little difference before the yielding of rebar. Therefore it comes to an important conclusion that for a given RC beam with the same material and geographic properties at each section, the load pattern and sensors placement have little influence on the average moment vs. macro-strain curves. In other words, if a presumption on uniformity is put forward to ensure that all of the physical parameters over the gauge length of a sensor (say a "cell", such as "cell3" in **Fig.12**) are homogeneous and only the average concepts like average moment, average curvature, average stiffness and so on are concerned, the moment-curvature analysis for one section based on fiber section model is suitable to deal with the relationship of various average parameters in each cell, which provides a valuable tool for the following inverse analysis on structural assessment.

(3) Deflection based on average stiffness in cells

Regarding the RC beam in **Fig.12** under load case1, suppose it is divided into several "cells" corresponding to the FBG sensor series and all the parameters in each cell are homogeneous. The deflection of the beam is investigated based on section fiber modeling. The moment-curvature curves for each section can be obtained in the same way as mentioned above. Then as two-point loading is applied, the average moment $\overline{M}(x)$ for each cell and the deflection of the full beam can be calculated based on conjugated method. Taking the P3(near 1/4 span) and P5(mid-span) in **Fig.12** for example, it can be found from **Fig.14** that the deflections based on the average stiffness match well with those originally calculated according to **Sec.4(3)**.

5. SHM STRATEGY FOR RC FLEXURAL STRUCTURE

All of the above discussions focus on the forward analysis in which the load and structural performance are known in advance and the structural responses (i.e. macro-strain measurements) are investigated. In the following section, some inverse problems including load identification and structural parametric estimation are studied. Finally, an integrated RC structural health monitoring strategy is proposed.

5.1 Inverse analysis

As mentioned in **Sec. 4(4)b**, each cell corresponding to the gauge length of a FBG sensor is assumed to share the common parameters in the average concept and can be treated as a fiber section model under a certain average moment. The forward analysis has shown that the load (equivalently, average moment) vs. macro-strain curves present a nice agreement with the analytic results which are calculated based on the known material and geometric properties. Therefore, the following discussions on the inverse problem achieve the verifications experimentally and analytically and will be extended in view of the average concepts concerning a cell.

(1) Load level identification

Load level identification is essential in some cases such as the vehicle load in bridge deck or the uncertainty of structural constraint and boundary condition. The load identification scheme is illustrated in **Fig.15**. Here the load to be identified is the average moment for a cell. Suppose the structural

physical parameters including material properties (concisely MP) and geometric properties (concisely GP) are known, the average curvature can be calculated based on the measured macro-strains at the bottom of the beam. Then from **Eq. (3)** based on the assumption of plane section, the strains over the height of the section can be obtained and the average moment can be identified.

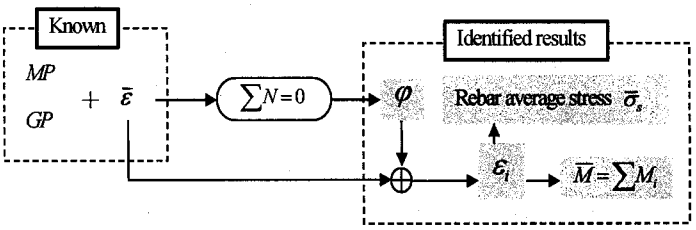

Fig.15 Load identification

(2) Structural parametric estimation

The estimation on structural performance is essential for structural health monitoring. Although structural parameters include many contents, technically if the loads and macro-strain responses are given in advance, one unknown structural parameter can be uniquely determined. Here considering the possible damage of a RC structure in practice, two parameters are chosen to be identified. One is the crossing area of reinforcing steel concerning to the corrosion, and the other is the compressive strength of concrete.

Crossing area of reinforcing steel **Fig.16** gives an illustration of the estimation on the crossing area and stress of reinforcing steel. As shown in **Fig.10**, calculating average moment with reference to *Y1* axis (the position of the object rebar) can avoid the unknown parameter and obtain the average curvature. The strains over the height of the section can be then calculated similarly. The crossing area and stress of reinforcing steel can be obtained based on the force equilibration.

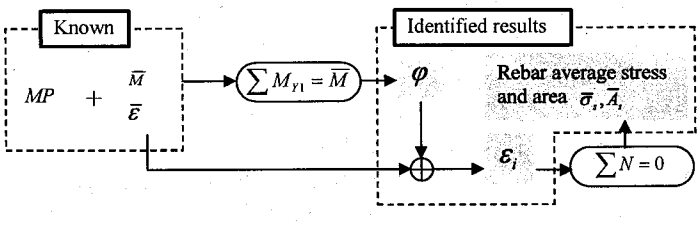

Fig.16 Estimation on rebar stress and crossing area

Compressive strength of concrete It can be found from **Eq. (1)** that in each stage of the constitutive model the compressive strength of concrete f_c acts as a coefficient. For the convenience of statement, suppose the **Eq.(1)** to be expressed as

$$\sigma = f_c \cdot g(\varepsilon) \tag{6}$$

Submitting **Eqs. (3) (6)** into **Eqs. (4) (5)** can lead to

$$\sum N = \sum_{i=1}^{n} f_c \cdot g\left(f(\varphi, \bar{\varepsilon}, Z_i)\right) A_i + \sigma_s A_s + \sigma_s' A_s' = 0 \tag{7}$$

$$\sum M = \sum_{i=1}^{n} f_c \cdot g\left(f(\varphi, \bar{\varepsilon}, Z_i)\right) Z_i + \sigma_s' A_s' \left(\frac{h}{2} - a'\right) + \sigma_s A_s \left(\frac{h}{2} - a\right) = \bar{M} \tag{8}$$

Therefore based on **Eqs. (7) and (8)**, the two unknowns φ, f_c can be determined uniquely.

5.2 RC SHM strategy

By summarizing all the discussions mentioned above, an integrated SHM strategy for RC flexural structures based on the developed long-gage fiber optic sensors array is proposed in **Fig.17**, which can be described as follows:

(Ⅰ) First of all, a numerical model (IM) is set up for the real structure. Generally it is possible to carry out controlled static tests before the structure is put into operation. The macro-strain measurements can be hence obtained with high precision, based on which the IM can be updated to provide a baseline with known structural physical parameters.

(Ⅱ) Taking a typical cell (*cell i*) corresponding to the i^{th} FBG sensor for example, structural damage identification as one main concern can be performed in two levels including crack monitoring and parametric estimation, which will be elaborated in (Ⅲ) and (Ⅳ) respectively.

(Ⅲ) Regarding the discussions in **Sec.3.2(1)**, local cracks can be successfully monitored including detect the occurrence, location and average crack width.

(Ⅳ) When it comes to structural parametric estimation, the determination of load is very important. If the controlled static tests can be implemented again, this issue will be easy and the reliable results may be obtained. However, it is often difficult to halt the working state of a structure in service and real-time monitoring is crucial. In such case, the average moment $\bar{M}_i$ for *cell i* can be first estimated in virtue of statistical measurements and the argument in **Sec.5.1(1)** on the assumption that there is no damage

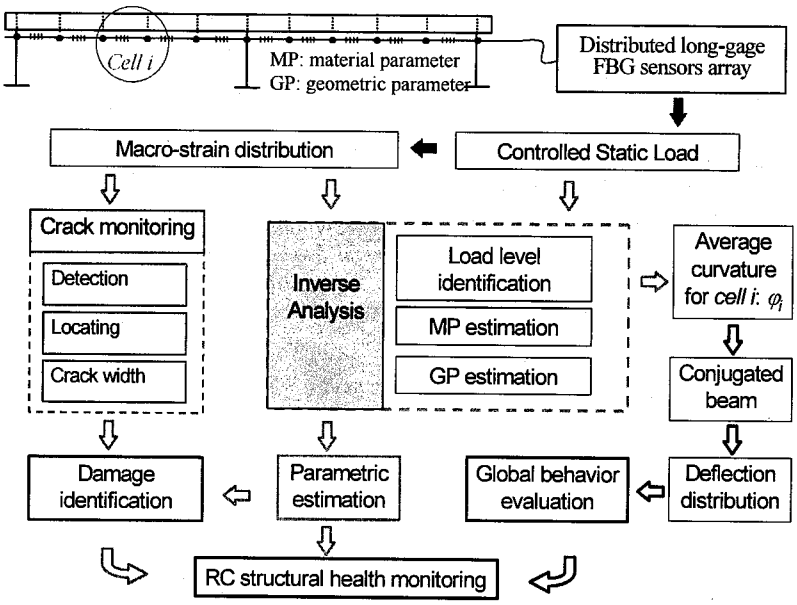

induced to the structure in the initial serving time. Suppose the statistical $\overline{M}_i$ is a constant in view of long-term behavior and then it can be used for structural parametric identification based on the discussion in **Sec.5.1(2).**

(V) By recalling the schemes in **Sec.5.1** inverse analysis, it can be found that the average curvature φ is an essential parameter and can be determined uniquely. Therefore the curvature distribution over the length of the beam can be obtained from FBG sensors array. Based on the conjugated beam method in **Sec.4.4(3)**, the deflection distribution of the beam may be calculated and the global structural behavior evaluation can be implemented as the other main concern.

6. CONCLUSIONS AND SUGGESTIONS

In this paper, based on the results from experiments and simulations, the application of the recently developed long-gage FBG sensor in health monitoring for RC flexural structures including local crack monitoring, parametric estimations and global behavior evaluation is investigated. Some important conclusions can be drawn as follows:

(1) The distributed long-gage FBG sensors can detect the occurrence and extent of cracks effectively. In general, the shorter the sensor gauge length is, the more evident the indication of crack initiation detection is. However, it is crucial to select an appropriate gauge length for practical application of such sensors in local crack monitoring.

(2) The FBG sensor with an adequate gauge length can obtain the measurements overlooking the influence of local cracks and providing the macro-information.

(3) As the gauge length and location of the FBG sensor is selected reasonably, the macro-strain vs. displacement curve presents a perfect linear correlation and hence the long-gage sensor may be supposed to replace the displacement transducer, which is often used for global deflection measurements but difficult to be installed onto the practical civil structures due to the requirement for a baseline position.

(4) The utilization of the distributed FBG sensors of 200mm gauge length is a good choice for a normal RC beam of about 2m span on both local crack monitoring and global behavior evaluation.

(5) A RC structure can be artificially divided into several "cells" corresponding to FBG sensor arrays and treated as a fiber section model, which has a clear expression on the relation of load, structural physical parameters and macro-strain measurements.

(6) The inverse analysis on load identification or parametric estimation can be implemented based on the conclusion (5) and the integrated strategy on RC SHM is put forward concerning (a) local damage identification including crack monitoring and parametric estimation and (b) global behavior evaluation in terms of structural deflection distribution.

(7) So far, this strategy is only suitable for new-built structures, i.e., those equipped with sensing system since construction. The further investigations should be considered for old and more complicated structures. The optimal sensor gauge length and placements also need to be

studied.

REFERENCES

1) W.L.Schulz, J.P.Conte, Eric Udd & M.Kunzler, 2002. Real-time damage assessment of civil structures using fiber grating sensors and modal analysis, *Proc. of SPIE vol.4696*
2) L.Q.Tang et al., 2003. Internal health monitoring of pre-stress beams of a bridge by FBGs, *Proc. of the first Structural Health Monitoring and Intelligent Infrastructure, Tokyo, Japan: 315-319, 2003*
3) Ansari F.,2003. Fiber optic health monitoring of civil structures, *Proceedings of the first Structural Health Monitoring and Intelligent Infrastructure, Tokyo, Japan: 19-30*
4) S.Z.Li and Z.S.Wu, 2005. Characterization of long-gage fiber optic sensors for structural identification, *Proc. of SPIE's Smart Structures & Materials and Nondestructive Evaluation for Health Monitoring & Diagnostics Symposium*, 2005
5) Zhishen Wu and Suzhen Li, 2005. Structural damage detection based on smart and distributed sensing technologies (Keynote), *Proc. of the 2nd International Conference on Structural Health Monitoring of Intelligent Infrastructure, 2005, pp107-120.*

(Received: July 10, 2007)